Marine Pollution Bulletin 208 (2024) 116968

Contents lists available at ScienceDirect

Marine Pollution Bulletin

journal homepage: www.elsevier.com/locate/marpolbul

Ecotoxicological effects of suspended sediments on marine microalgae using flow cytometry and pulse-amplitude modulation (PAM) fluorometry

Shin Yeong Park [a], Junghyun Lee [b,*], Inha Kwon [a], Hyunseo Song [a], Beomgi Kim [a], Taewoo Kim [a], Changkeun Lee [a], Seo Joon Yoon [a], Junsung Noh [c], Seongjin Hong [d], Jong Seong Khim [a,*]

[a] School of Earth and Environmental Sciences & Research Institute of Oceanography, Seoul National University, Seoul 08826, Republic of Korea
[b] Department of Environmental Education, Kongju National University, Gongju 32588, Republic of Korea
[c] Department of Environment & Energy, Sejong University, Seoul 05006, Republic of Korea
[d] Department of Marine Environmental Sciences, Chungnam National University, Daejeon 34134, Republic of Korea

ARTICLE INFO

Keywords:
Suspended sediment
Microalgal bioassay
Flow cytometry
PAM fluorometry
Ecotoxicological effects

ABSTRACT

Microalgal bioassays were conducted to evaluate the ecotoxicological effects of suspended sediments (SS) collected from coastal environments. Growth inhibition was assessed for six microalgal species, and multiple endpoints were measured using flow cytometry (FCM) and pulse-amplitude modulation (PAM) fluorometry for three species (*Dunaliella tertiolecta*, *Isochrysis galbana*, and *Phaeodactylum tricornutum*). Among these, the EC50 for growth inhibition of *D. tertiolecta* (6700 mg L^{-1}) was notably lower compared to the other species, and among several endpoints, esterase activity was the most inhibited. Species-specific responses to SS exposure were identified, with *D. tertiolecta* exhibiting greater susceptibility across most endpoints. Meanwhile, measurements of Fo', Fm', and Y(NPQ) in *P. tricornutum* using PAM fluorometry revealed greater sensitivity. Based on the results of this study and review, the tentative predicted no-effect concentration was calculated as 12.1 mg L^{-1}. Overall, this study provides novel insights into SS ecotoxicity, establishing a crucial baseline for future investigations.

1. Introduction

Suspended sediments (SS) frequently occur in high concentrations in the water column due to various natural processes and anthropogenic activities such as sand mining (Newcombe and MacDonald, 1991; Hackney et al., 2021; Dethier et al., 2023). Specifically, sand mining to procure sand as a construction material has emerged as a persistent global environmental issue (Asabonga et al., 2017; Da and Le Billon, 2022). In marine environments, SS is known to induce respiratory complications or evasive behavior in organisms, potentially resulting in community-level impacts after long-term exposure (Pollock et al., 2014). Previous studies have evaluated the adverse effects of SS on fish and bivalves (Chu et al., 2020; Elfwing and Tedengre, 2002), revealing effects on immune responses, food intake, as well as growth and survival rates of some marine invertebrates and fish (Utne-Palm, 2002; Wenger et al., 2012). However, *Nannochloropsis oculata* was the only report on the effect of SS on microalgae (MOF, 2016).

Damage to microalgae, which play a crucial role in marine ecosystems as primary producers, can disrupt the ecological balance and have adverse effects on higher trophic-level organisms, such as zooplankton and fish (Nestler et al., 2012). Due to their rapid growth rate and high sensitivity to pollutants (Bauer et al., 2012), microalgae are considered essential indicators in ecotoxicity assessments. While microalgal bioassays are commonly used to evaluate pollutant toxicity, there has been limited research on the effects of physical particles like SS. It is crucial to establish suitable endpoints for assessing microalgal damage caused by SS.

Traditionally, microalgal bioassays have primarily focused on growth inhibition endpoints, as the growth rate serves as an integrative measure reflecting interference in multiple intracellular processes. International standard guidelines presented by the American Society for Testing and Materials (ASTM) and the International Organization for Standardization (ISO) also provide only for growth inhibition (ASTM, 2012; DIN EN ISO10253, 2018). Analyzing a single endpoint cannot provide insights into the mechanism underlying responses of microalgae to stressors (Esperanza et al., 2015). Recent technological advancements have enabled the evaluation of various endpoints in microalgae through the use of flow cytometry (FCM) and pulse amplitude modulation (PAM)

* Corresponding authors.
E-mail addresses: leejunghyun@kongju.ac.kr (J. Lee), jskocean@snu.ac.kr (J.S. Khim).

https://doi.org/10.1016/j.marpolbul.2024.116968
Received 25 April 2024; Received in revised form 8 August 2024; Accepted 8 September 2024

fluorometry (Lee et al., 2023). FCM is a valuable method for rapidly assessing the metabolic state of microalgal cells, offering multiple fluorometric and light-scattering parameters for individual cells. This approach effectively enables the determination of the impact of various compounds on microalgal species (Franklin et al., 2001; An et al., 2021). In addition, the assessment of chlorophyll (Chl) fluorescence via PAM fluorometry, which involves imaging Chl fluorescence in microalgal samples, allows for rapid and accurate measurement of toxicity to plants across multiple samples (Schreiber et al., 2007). This technique has been applied to analyze the toxicity of various substances, including metals, herbicides, gamma rays, and nanoplastics, to microalgae (Almeida et al., 2017; Almeida et al., 2019; Gomes et al., 2020).

This study aimed to identify specific toxic effects induced by SS generated from sand mining on marine microalgae. The specific objectives were to: (1) evaluate the impact of SS on the growth inhibition of six microalgae (green algae; *Dunaliella tertiolecta* and *Tetraselmis striata*, haptophytes; *Isochrysis galbana*, diatoms; *Skeletonema costatum* and *Phaeodactylum tricornutum,* and raphidophytes; *Heterosigma akashiwo*); (2) investigate the effect of SS on various parameters of three selected marine microalgae, encompassing chlorophyll-*a* (Chl-*a*) content, esterase activity, cell membrane integrity, cell size, and intracellular complexity; (3) examine the effect of SS on the photosystem II (PSII) performance in microalgae; (4) identify the most sensitive endpoints on microalgae; and (5) evaluate the ecological risk posed by SS to the marine ecosystem by deriving the interim-predicted no-effect concentration (PNEC).

2. Materials and methods

2.1. Cultivation of microalgae

To investigate the ecotoxicological effects of SS exposure on microalgae, we tested various taxa, including two species each of diatoms, green algae, and flagellates. The diatoms were *P. tricornutum*, an international standard test species recommended by ASTM and ISO (ASTM, 2012; DIN EN ISO10253, 2018), and *S. costatum*, commonly found in coastal ecosystems (Yamada et al., 2013). For green algae, we selected *D. tertiolecta*, another international standard test species, and *T. striata*, a marine microalga widely distributed worldwide and adaptable to various nutrient conditions (Patrinou et al., 2023). The flagellates selected were *H. akashiwo*, a red tide-causing species and important model organism for evaluating responses to environmental changes (Wang and Liu, 2022), and *I. galbana* is widely used in microalgal bioassays due to its high sensitivity (Lee et al., 2020). *D. tertiolecta* was obtained from NeoEnBiz Inc. (Bucheon, Korea), and the other microalgae were obtained from the Korea Marine Microalgae Culture Center (KMMCC, KIOST, Geoje, Korea).

Microalgae were cultured according to DIN EN ISO10253 (2018), with some modifications (DIN EN ISO10253, 2018). In brief, microalgae were cultivated in 250 mL culture flasks, starting with initial densities of 3.0×10^4 cells mL^{-1} for *D. tertiolecta*, 9.0×10^4 cells mL^{-1} for *I. galbana*, 7.0×10^4 cells mL^{-1} for *P. triconutum*, and 5.0×10^4 cells mL^{-1} for *T. striata*, *H. akashiwo*, and *S. costatum* in f/2 medium. To obtain accurate and meaningful results, we used initial cell densities higher than those generally recommended in DIN EN ISO10253 (2018). The initial concentrations of six microalgal species were adjusted based on their specific growth characteristics and sensitivity to SS. Our preliminary experiments identified the initial cell densities at which each species could reach the exponential growth phase within 3–4 days of cultivation. Previous studies have also shown that different microalgal species exhibit optimal growth and sensitivity responses at varying initial concentrations (1.5×10^4–2.0×10^6 cells mL^{-1}) (Schüler et al., 2021; Wang et al., 2013; Yamasaki et al., 2018). Furthermore, higher initial cell densities are necessary to obtain reliable and reproducible data for evaluating multiple endpoints, such as esterase activity, cell membrane integrity, and intracellular complexity, in addition to growth inhibition (An et al., 2021).

2.2. Sampling and sample preparation

SS were collected in May 2022 from the sand mining complex in the exclusive economic zone of the West Sea in South Korea. The sediments were transported to the laboratory and subjected to wet-sieving using a 63-μm mesh sieve to obtain fine particles, as SS particles are defined as being <63 μm (Garcia, 2008).

The supernatant was removed and stored at −4 °C to prevent changes in the biochemical properties of the sediment. For the analysis of SS, both particle size distribution and metals (Cd, Cr, Cu, Ni, Pb, Zn, As, and Hg) concentrations were analyzed. Concentrations of metals were analyzed using an Elan 6100 inductively coupled plasma-mass spectrometer (ICP-MS, Perkin-Elmer SCIEX, Norwalk, CT, USA).

2.3. Exposure of samples to microalgae

Bioassays of microalgae exposed to SS followed the methods of previous studies (DIN EN ISO10253, 2018; Lee et al., 2020) with some modifications (Fig. 1a and Table S1). Algae in the exponential growth phase were used for the bioassays and were cultured for 72–96 h. The SS concentration ranged from 0 (control) to 100, 500, 1000, 5000, and 10,000 mg L^{-1}, using f/2 culture medium. The reported highest concentration of SS in the sand mining complex was 7200 mg L^{-1}, which decreased to 17 mg L^{-1} when dispersed approximately 5 km (Nichols et al., 1990). Thus, the chosen concentration range of SS was designed to encompass this reported variability to provide comprehensive coverage for potential environmental scenarios. All experiments, including a control group, were performed in triplicates. To maintain the SS concentration, culture flasks were positioned horizontally in the incubator and shaken at 100 rpm throughout the 0–96 h exposure period to ensure stability of SS concentration (Joshi et al., 2023). Random flask repositioning was conducted every 24 h to minimize potential variations in lighting intensity. The culture conditions were maintained at a temperature of 20 ± 1 °C, with a light intensity of 100 μmol photons m^2 s^{-1} provided by cool white fluorescent lamps on a 12:12 h light-dark cycle. The seawater salinity was kept at 30 practical salinity units, and the pH was maintained at 8.0 ± 0.2.

2.4. Growth inhibition of microalgae

After 96 h of exposure, cell numbers were quantified using a disposable hemocytometer (INCYTO, Cheonan, Korea) and an Olympus CKX53 microscope (Olympus Corporation, Tokyo, Japan) to assess the intrinsic growth rate (μ) and growth inhibition ($I_{\mu i}$). Eq. (1) represents the estimation of these parameters, where N_0 signifies the initial cell density, and N_{96} represents the cell density at 96 h. Eq. (2) defines μ_i as the growth rate of culture flask 'i', while 'μ_C' denotes the average growth rate of the control group (DIN EN ISO10253, 2018).

$$\mu = \frac{\mathrm{In}\,(N_{96}) - \mathrm{In}(N_0)}{t_{96}} \quad (1)$$

$$I_{\mu i}(\%) = \frac{\mu_c - \mu_i}{\mu_c} \times 100 \quad (2)$$

2.5. Flow cytometry analysis

FCM analysis was carried out using a FACS Canto II flow cytometer (BD Biosciences, San Jose, CA, USA), equipped with three lasers (405, 488, and 633 nm) and eight filters. The staining method and conditions used to observe each endpoint were based on the description by Lee et al. (2015), with some modifications (Table S2). Briefly, fluorescence corresponding to high Chl-*a* content was measured using a 633 nm laser, while cell size and intracellular complexity were measured using a 488

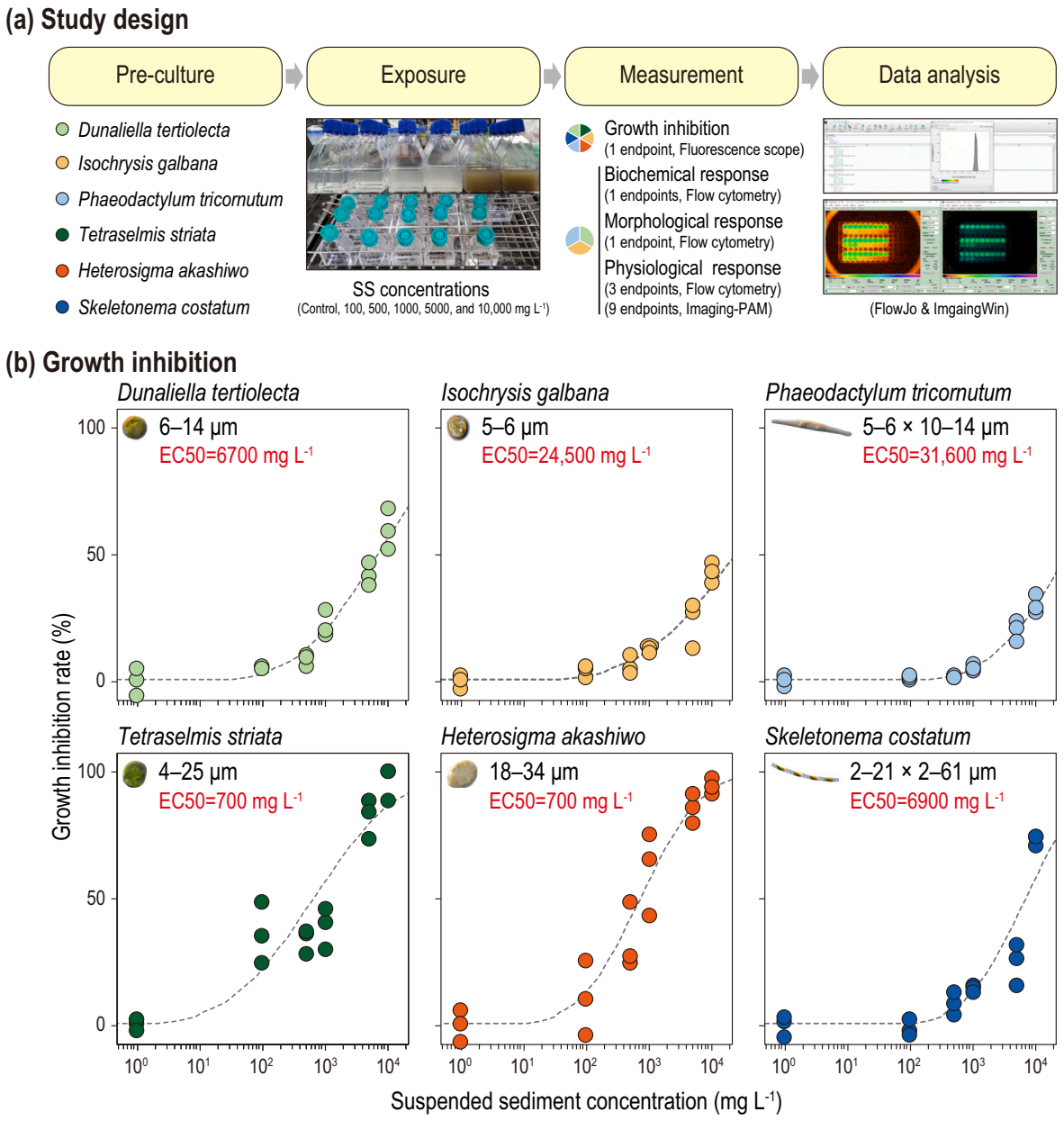

Fig. 1. (a) Scheme of present study. Growth inhibition was measured in all six species (*Dunaliella tertiolecta*, *Isochrysis galbana*, *Phaeodactylum tricornutum*, *Tetraselmis striata*, *Heterosigma akashiwo*, and *Skeletonema costatum*) of microalgae, while other endpoints were exclusively measured in *D. tertiolecta*, *I. galbana*, and *P. tricornutum*. (b) Growth inhibition rates and calculated effective concentrations (EC50s) of six species of microalgae after exposure to six concentrations of suspended sediment (0 to 100, 500, 1000, 5000, and 10,000 mg L^{-1}).

nm laser with forward and side scatter detectors, respectively (Table S2). To assess esterase activity and cell membrane integrity, *I. galbana* was double-stained with FDA and SYTOX Blue (Lee et al., 2020). This dual-staining method allows for the simultaneous measurement and interpretation of various cell characteristics. The positions of the dot plots (Q1–Q4) indicated by dual-staining are described in Fig. S1 and Table S3. In contrast, *D. tertiolecta* and *P. tricornutum* were evaluated for membrane integrity by single-staining with PI (Fig. S1), which has been more widely used in previous studies (Wei et al., 2014; Wang et al., 2023), due to potential emission overlap between FDA and PI (Olsen et al., 2016).

2.6. PAM fluorometer analysis

PAM fluorometer (IMAGING-PAM, Heinz Walz GmbH, Effeltrich, Germany) in conjunction with the ImagingWin software (Heinz Walz GmbH PAM, Effeltrich, Germany) was employed to assess the PSII performance in microalgae under SS exposure, following the method described by Almeida et al. (2019). After 96 h of SS exposure, *D. tertiolecta*, *I. galbana*, and *P. tricornutum* cells were centrifuged at 4200 rpm for 15 min. Subsequently, the resulting pellets were resuspended in ISO medium. A 200 μL aliquot from each replicate sample was transferred to a 96-well microplate (Costar®; Corning Incorporated, NY, USA), and Chl-*a* fluorescence was measured.

Following the determination of minimum and maximum PSII fluorescence yields (Fo and Fm, respectively), microalgal cells that had been dark-acclimated were exposed to light (~80 μmol m^{-2} s^{-1}). Fluorescence yield (Ft) in the light, namely the minimum fluorescence yield (Fo') and maximum fluorescence yield (Fm') in the light-adapted state were recorded. Seven parameters, including the effective PS II quantum

yield (Y(II)), quantum yield of regulated energy dissipation (Y(NPQ)), quantum yield of non-regulated energy dissipation (Y(NO)), coefficient of photochemical quenching (qP and qL), coefficient of non-photochemical quenching (qN), and maximum photosynthetic electron transport rate ($_{max}$ETR), were measured. All endpoints analyzed using Imaging-PAM were quantified based on formulas provided in Table S4.

2.7. Data analysis and statistics

To determine the half-maximal effective concentrations (EC50s) of SS and perform statistical analysis, SPSS 24.0 (SPSS Inc., Chicago, IL, USA) was employed. In order to comparatively assess the impact of SS among different treatment groups, fold induction was calculated as the ratio of each endpoint result from the treatment group to that of the control group. Principal components analysis (PCA) was conducted to interpret and visually represent the results of microalgal endpoints, utilizing PRIMER v6 software (PRIMER-E Ltd., Plymouth, UK).

The PNEC was determined using the species sensitivity distribution (SSD) method (Gredelj et al., 2018; Gao et al., 2014). SSD analysis involved log-transformed toxicity data derived from EC50 and LC50 values and was carried out using R studio (PBC, Boston, MA, USA). Chronic data for EC50 and LC50 were obtained by applying an acute-chronic ratio (ACR) of 10 (Chapman et al., 1998). The SSD curve was constructed using lognormal statistical distribution, a widely accepted and simple model that is consistent with findings from other studies (Gao et al., 2014; Xu et al., 2015). PNEC values are generally associated with the hazardous concentration for 5 % of the species (HC5), and HC5 values were also calculated using R studio. To address the remaining uncertainty in the estimated threshold, HC5 was divided by the additional assessment factor (AF) to derive the final PNEC (the highest AF 5 is the default value) (Amiard and Amiard-Triquet, 2015; EC, 2011).

3. Results and discussion

3.1. Growth inhibition of microalgae

The growth inhibition rates of the six microalgae exhibited an increasing trend with higher concentrations of SS (Fig. 1b). Interestingly, at the lowest SS concentration (100 mg L^{-1}) in this study, a growth stimulation of approximately 5 % was observed across all species. This phenomenon is believed to be the hormesis effect, as documented in previous studies, where low concentrations of toxic substances promote the growth of microalgae (Lee et al., 2020). While the mechanisms of influence from toxic substances and SS might differ, it is supposed that the substances present in SS, such as organic matter and metals, can promote the growth of microalgae.

At the highest SS concentration (10,000 mg L^{-1}), all microalgae experienced a significant inhibition in growth, ranging from 67 % to 97 %. This inhibition could be attributed to metals in SS (Overnell, 1975), but it could also be due to the shading effect that reduces the availability of light for photosynthesis. To address this concern, the concentrations of nine metals in the SS were analyzed. All elements, including As, Cr, Cu, Li, Ni, Pb, Zn, Cd, and Hg, did not exceed sediment quality guidelines, including threshold effect level, probable effect level, effect range low, and effect range median (Long et al., 1995; Long and MacDonald, 1998). Additionally, even when considering their potential dissolution in seawater, it was determined that the concentrations did not exceed water quality guidelines (except for Pb concentration in the highest SS concentration) (MOF, 2018) (Table S5). While other potentially hazardous compounds might be present, as these are generally less soluble in seawater than metals (Duce et al., 1991), this study assumed that their effects were negligible. Thus, it is suggested that the growth inhibition of microalgae might be more affected by the shading effect, which is particularly prominent at higher SS concentrations (Yeh et al., 2011).

The calculated EC50s for the six species ranged from 700 to 3.16 × 10^4 mg L^{-1}, in the following order: *T. striata*, *H. akashiwo*, *D. tertiolecta*, *S. costatum*, *I. galbana*, and *P. tricornutum* (Fig. 1b). In addition to SS, *Tetraselmis* sp. is known to be sensitive to environmental pollutants, such as polycyclic aromatic hydrocarbons, including phenanthrene, naphthalene, and anthracene (Vieira and Guilhermino, 2012), as well as metals, such as Cu and Zn (Li et al., 2017; Liu et al., 2011). *Tetraselmis* sp. are industrially important green marine microalgae that are used extensively in aquaculture feeds due to their accumulation of polyunsaturated fatty acids, particularly omega-3 fatty acids (Schulze et al., 2019). Thus, efficient cultivation and management of *Tetraselmis* sp., maintaining appropriate SS concentration should be considered. In contrast, *H. akashiwo*, one of the most sensitive species to SS, is a harmful algal bloom species known for producing biotoxins that can harm other marine organisms and pose threats to human health (Imai et al., 2021). While the presence of SS is believed to contribute to the reduction of *H. akashiwo* blooms due to anthropogenically induced environmental changes, excessive SS stress might lead to the overproduction of biotoxins. This necessitates careful management to balance the benefits and risks associated with SS exposure.

The species exhibited different sensitivity to SS, with green algae showing greater sensitivity compared to diatoms. In general, the insensitivity of diatoms can be attributed to the presence of a cell wall (Ene et al., 2015). Diatoms are commonly known to form silicified frustules in response to elevated concentrations of toxic substances, such as ammonia, hydrogen sulfide, and metals in sediments, providing them with high resistance (Metaxas and Lewis, 1991; Kwon, 2013). However, certain diatoms, such as *P. tricornutum*, can resist environmental toxicants even without forming silicified frustules (Chuang et al., 2014). This resistance might explain why *P. tricornutum* shows relatively lower sensitivity to SS.

3.2. Inherent properties and viability of microalgae

Esterase activity was affected in all three microalgae exposed to SS (Fig. 2a). In the case of *I. galbana*, an increase in SS concentration led to a gradual decrease in the percentage of healthy cells (% control gate), reaching 0.40 % at the highest SS concentration. In particular, *I. galbana* exposed to SS showed not only inhibition of esterase activity but also alterations in cell membrane integrity. The population of *I. galbana* in Q4 on the dot plot, representing cells affected by both inhibition of esterase activity and changes in cell membrane integrity, ranged from 1.3 % to 12 %. For *D. tertiolecta*, esterase activity gradually decreased with increasing SS concentration, reaching 0.02 % of control cells at the highest SS concentration. In contrast, for *P. tricornutum*, esterase activity was 53 % of the control at the lowest SS concentration and exhibited minimal variation with increasing SS concentrations. Esterase, a crucial enzyme for phospholipid regeneration (Franklin et al., 2001), plays a pivotal role in maintaining microalgal biomass. Although esterase is not directly involved in photosynthesis, its activity serves as an indicator of cell metabolic activity and viability (Afrimzon et al., 2008). When microalgae are exposed to SS, decreased esterase activity indicates cellular stress and potential metabolic disruption. This suggests that elevated SS concentrations might adversely affect the health and viability of marine microalgal populations, highlighting the ecological risk of SS contamination. Future studies measuring RuBisCO and carbonic anhydrase could provide a more comprehensive understanding of the impact of SS on photosynthesis.

SS exposure also resulted in damage to cell membrane integrity in *I. galbana*, while *D. tertiolecta and P. tricornutum* showed little damage (Fig. 2a). Since cell membrane integrity is closely related to cell viability and division ability (Machado and Soares, 2012) in microalgae growth, a decline in membrane integrity might lead to apoptosis and programmed cell death (Gallo et al., 2017). The intracellular complexity showed a noticeable increase in *D. tertiolecta* and *I. galbana* (Fig. S2). Active cells tend to enlarge before dividing due to the increase in cellular constituents, and this active metabolism could be reflected in the increased cellular complexity (Míguez et al., 2021). Further research is

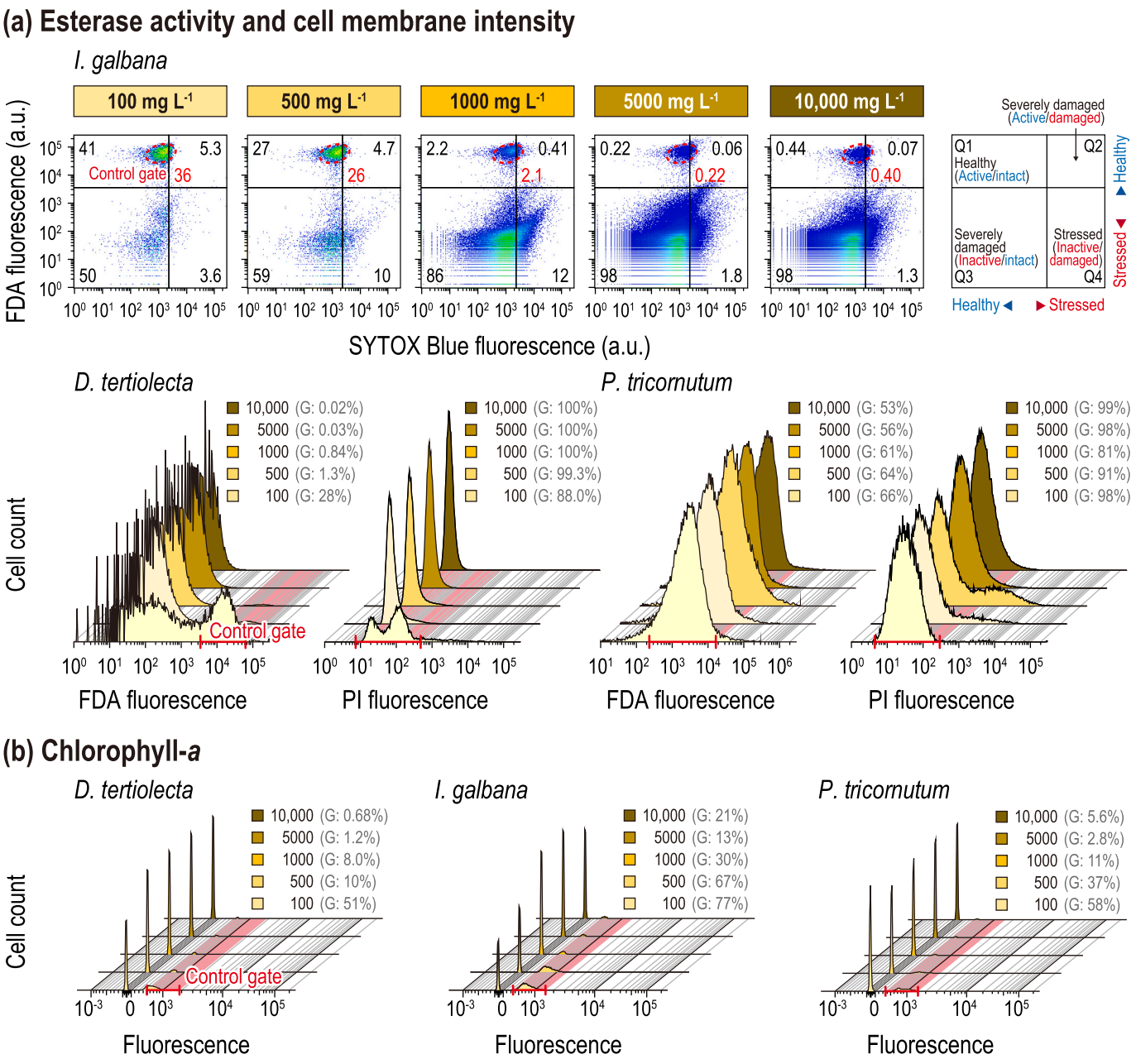

Fig. 2. Results of microalgal assays after exposure to the suspended sediment. (a) Flow cytometry dot plots of *Dunaliella tertiolecta* and *Isochrysis galbana* cells with FDA and SYTOX blue, and fluorescence histograms for *Phaeodactylum tricornutum* cells with FDA and PI. (b) Fluorescence histograms for chlorophyll-*a* measurement in *D. tertiolecta*, *I. galbana*, and *P. tricornutum*. (For interpretation of the references to colour in this figure legend, the reader is referred to the web version of this article.)

needed to elucidate the observed changes in cell size without corresponding alterations in intracellular complexity.

Chl-*a* fluorescence significantly decreased with increasing SS concentrations in all three species (Fig. 2b). In *D. tertiolecta*, Chl-*a* fluorescence was reduced by nearly 99 % at the highest SS concentration. Similarly, *I. galbana* and *P. tricornutum* exhibited Chl-*a* reduction rates of 76 % and 92 %, respectively, at the highest SS concentration. The inhibition of Chl-*a* fluorescence may be associated with potential damage to photosystem II (PSII) or changes in the Chl-*a* content, affecting the photosynthetic process (Overnell, 1975). The relationship between photosynthesis and growth inhibition has been previously reported, and this inhibition can lead to chronic toxicity (Magnusson et al., 2008; Wang et al., 2020); our results suggest that exposure to SS for 96 h can induce chronic toxicity.

3.3. PSII efficiency of microalgae

Given that the Chl-*a* content is the endpoint most significantly affected by the exposure of microalgae to SS, SS exposure likely has a substantial impact on the photosynthetic ability of microalgae. The Fo' and Fm' values decreased significantly with increasing SS concentration in all three species (Fig. 3). This decrease is believed to result from a reduction in the electron transport capacity of PSII (Ranjbarfordoei et al., 2006). The $_{max}$ETR decreased in all three species compared to the control up to an SS concentration of 500 mg L^{-1}, but then increased at concentrations above 1000 mg L^{-1} (Fig. S3). Decreases in $_{max}$ETR can impact PSII-PSI electron transport and all photosynthesis-related responses, thereby negatively affecting the physiological state of microalgae (Hess, 2000; Juneau and Popovic, 1999). The $_{max}$ETR increase to a

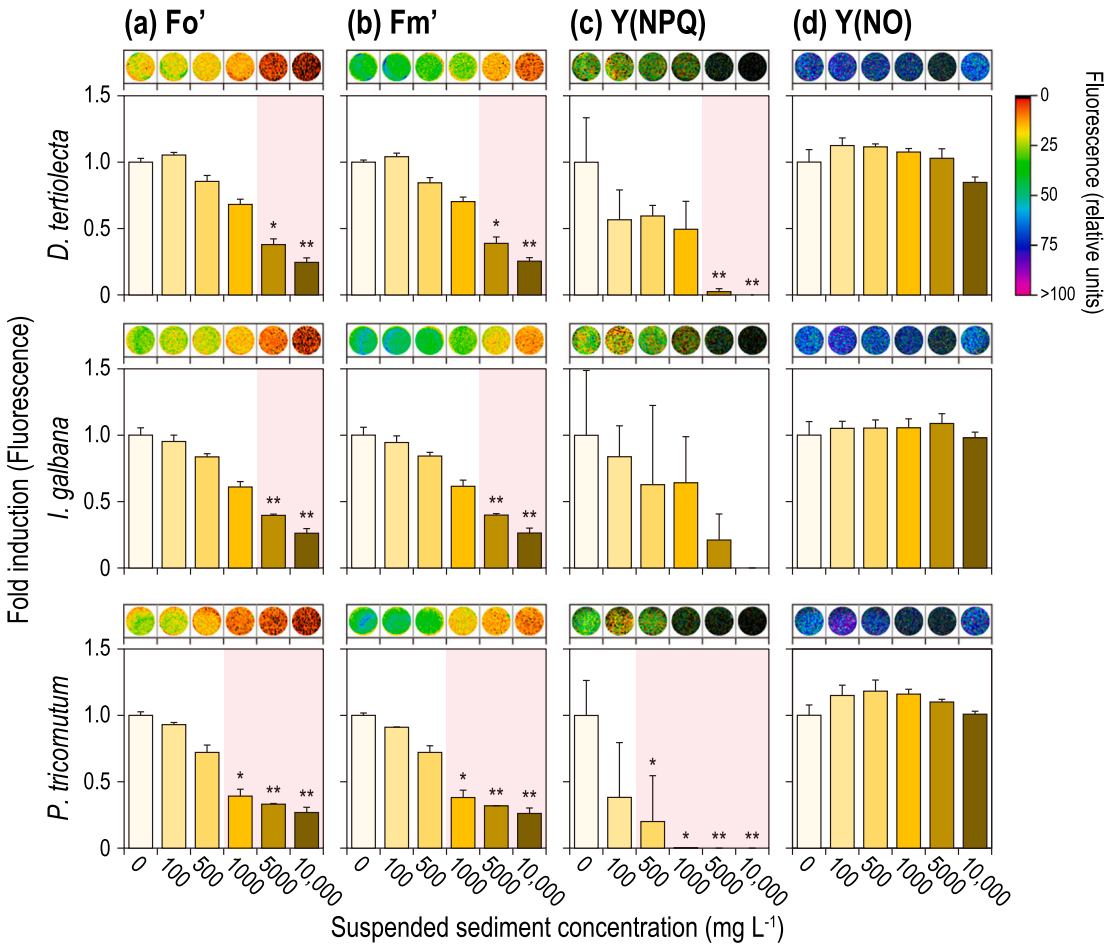

Fig. 3. Photosystem II parameters of *Dunaliella tertiolecta*, *Isochrysis galbana*, and *Phaeodactylum tricornutum* exposed to suspended sediments. (a) Fo' – Minimum fluorescence in light-adapted state; (b) Fm' – Maximum fluorescence in light-adapted state; (c) Y(NPQ) – Quantum yield of regulated energy dissipation; (d) Y(NO) – Quantum yield of nonregulated energy dissipation. All endpoints are expressed in fold induction for fluorescence. Data (mean ± standard deviation) represent results from three replicate experiments (* and ** represent significantly different compared by control $p < 0.05$ and $p < 0.01$, respectively). Red shading indicates a significant difference ($p < 0.05$) compared to the control group. (For interpretation of the references to colour in this figure legend, the reader is referred to the web version of this article.)

very high level with exposure to high SS concentrations may be attributed to a limitation of the imaging-PAM device, which can record a very high $_{max}$ETR value when the biomass is very low. Considering the pronounced decrease in Chl-*a*, Fo', and Fm' above 1000 mg L^{-1}, this limitation could be considered as an artifact of the device rather than an actual increase in $_{max}$ETR.

For all three microalgae, the Y(NPQ) exhibited a rapid decrease as the SS concentration increased (Fig. 3c). At the highest SS concentration, *D. tertiolecta* and *I. galbana* exhibited significant decreases in Y(NPQ) compared to the control, while *P. tricornutum* showed a 100 % decrease at an SS concentration of 1000 mg L^{-1}. Y(NPQ) represents the ratio that reduces light damage by emitting light energy as heat energy when photosynthetic organisms, such as microalgae, are exposed to stressors (Murchie and Lawson, 2013). Although NPQ generally increases in response to stress in organisms (Johnson et al., 1993), it continued to decrease due to SS exposure in the present study. This decrease in NPQ is believed to result from reduced activity in all photochemical processes (PSII and PSI) and the inhibition of photosynthetic electron transfer due to the decline in Chl-*a* fluorescence.

SS exposure did not have a significant effect on the Y(NO) (Fig. 3d). This result suggests that the protective regulatory mechanism, which converts the remaining light energy used in photosynthesis into photochemical energy, was insufficient to safeguard the microalgae (Almeida et al., 2021). Consequently, the microalgae struggle to cope with radiation and become photodamaged (Kramer et al., 2004). The decrease in Y(NPQ) and the slight increase in Y(NO) in all three microalgae species suggest that SS exposure reduces the mechanisms involved in photosynthesis, causing residual light energy to be released through photochemical reactions rather than thermal energy.

With SS exposure, qN values tended to decrease, while Y(II), qL and qP values tended to increase (Fig. S3). Although Y(II) was expected to decrease with SS exposure, an unexpected increase was observed. This irregularity might be due to limitations in the measurement device, which could artificially increase Y(II) values when the biomass is low. Beecraft et al. (2021) noted that ensuring the reliability of PAM measurements under low biomass conditions is challenging, which can lead to Y(II) values being measured higher than they actually are. Y(II) typically follows a similar pattern to $_{max}$ETR (Almeida et al., 2021), and given the observed increase in $_{max}$ETR due to device limitations, it remains uncertain whether Y(II) actually increased. Further studies are required to confirm this observed increase. The relative distribution of energy dissipation processes through PSII revealed that photochemical quenching was promoted to dissipate the excess of light energy. The decrease in qN value and the increase in qL and qP values due to SS exposure suggest that photochemical quenching is enhanced during the energy dissipation process through PSII, thereby dissipating excess light energy. However, this dissipation process may not be sufficient to prevent damage, and it is believed that photodamage and an increase in

reactive oxygen species will adversely affect microalgal growth.

3.4. Relationship between endpoints

In the results of PCA, the two axes for *D. tertiolecta*, *I. galbana*, and *P. tricornutum* explained 93 %, 95 %, and 93 % of the total data variance, respectively (Fig. 4a). PC1 for all three species exhibited a clear distinction between the low concentration group (0, 100, 500, and 1000 mg L^{-1}), including the control, and the high concentration group (5000 and 10,000 mg L^{-1}). Across all three species, esterase activity, Chl-*a* content, cell size, intracellular complexity, Fo', Fm', Y(NPQ), Y(NO), and qN were affected in the control and low concentration groups, whereas growth inhibition, Y(II), qL, qP, and $_{max}$ETR were affected in the high concentration group. These results suggest that measuring endpoints related to cell viability, rather than relying solely on traditional endpoints based on growth inhibition, can provide a more precise assessment of the effects of SS exposure. Given the observed correlations among these endpoints, it would be beneficial to select the most feasible endpoint for measurement (Tables S6–S8).

The average percentage variation in multiple endpoints of microalgae exposed to SS compared to the control is provided in Fig. 4b. Among the three species, *D. tertiolecta* exhibited sensitive responses in endpoints measured by FCM at relatively low SS concentrations, while *P. tricornutum* demonstrated sensitivity in endpoints measured by imaging-PAM. In contrast to *D. tertiolecta* and *P. tricornutum*, *I. galbana* showed a gradual increase in most physiological responses with increasing SS concentration. In bioassays with *D. tertiolecta*, the use of FCM is advantageous for obtaining a sensitive response, whereas for bioassays with *P. tricornutum*, imaging-PAM is more beneficial. The lower sensitivity of FCM for *P. tricornutum* may be attributed to the morphological characteristics of this microalgal species, as its fusiform or oval shape (Desbois et al., 2010) can lead to significant variations in FCM results. *I. galbana* proves well-suited for assessing the impacts of microalgae exposure to various pollutant concentrations, given its ability to confirm step-by-step responses in detail.

3.5. Species sensitivity distribution for SS

We constructed a SSD by reviewing studies on lethal SS concentrations for various biological taxa (Fig. 5). The HC5 in SS was derived as 61 mg L^{-1}, and a tentative PNEC, considering an AF, was then calculated as 12.1 mg L^{-1}. The most sensitive endpoint observed was the growth inhibition of *T. striata*, which fell below the HC5. As a result, we propose a tentative PNEC of 12.1 mg L^{-1} for SS. The PNEC value could be a recommended water quality standard for SS to protect marine organisms from SS generated during sand mining. In this study, we utilized only the EC50 for microalgal growth inhibition and the LC50 for other organisms to establish more robust standards. The primary reason for including toxicity data from freshwater organisms was the lack of marine-specific toxicity data for SS. This approach is supported by precedents where freshwater data has been used when marine data is scarce, as certain physiological and ecological responses to pollutants can be comparable between freshwater and marine species (Warne et al., 2018). Furthermore, we considered data solely for adult organisms, employing a

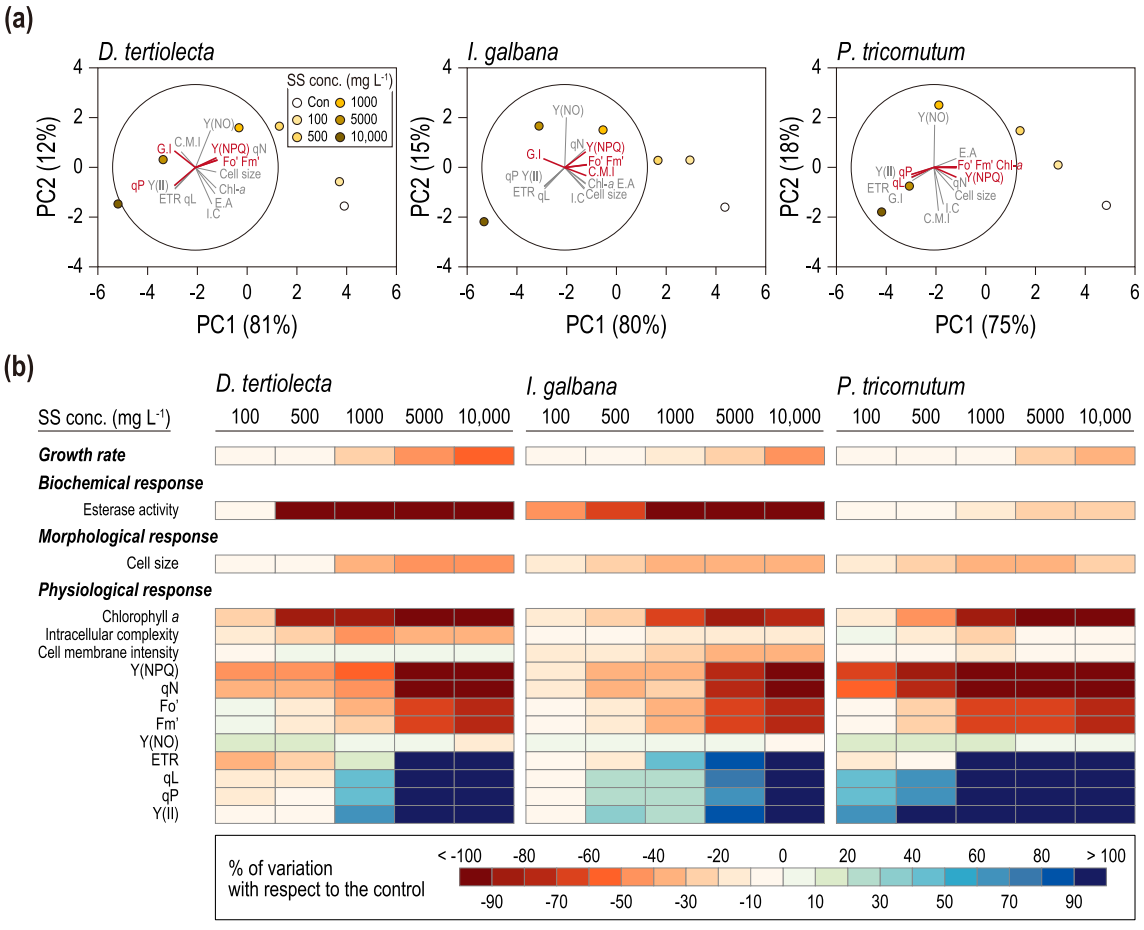

Fig. 4. (a) Principal component analysis (PCA) results for *Dunaliella tertiolecta*, *Isochrysis galbana*, and *Phaeodactylum tricornutum* exposed to suspended sediment (SS). The top 5 variables with high contribution in principal component 1 (PC1) are marked in red. Some variables are abbreviated (G.I: growth inhibition; E.A.: esterase activity; Chl-*a*: chlorophyll-*a* content; I·C: intracellular complexity; C.M.I: cell membrane integrity; ETR: electron transfer rate). (b) Average toxic responses induced by SS concentrations. (For interpretation of the references to colour in this figure legend, the reader is referred to the web version of this article.)

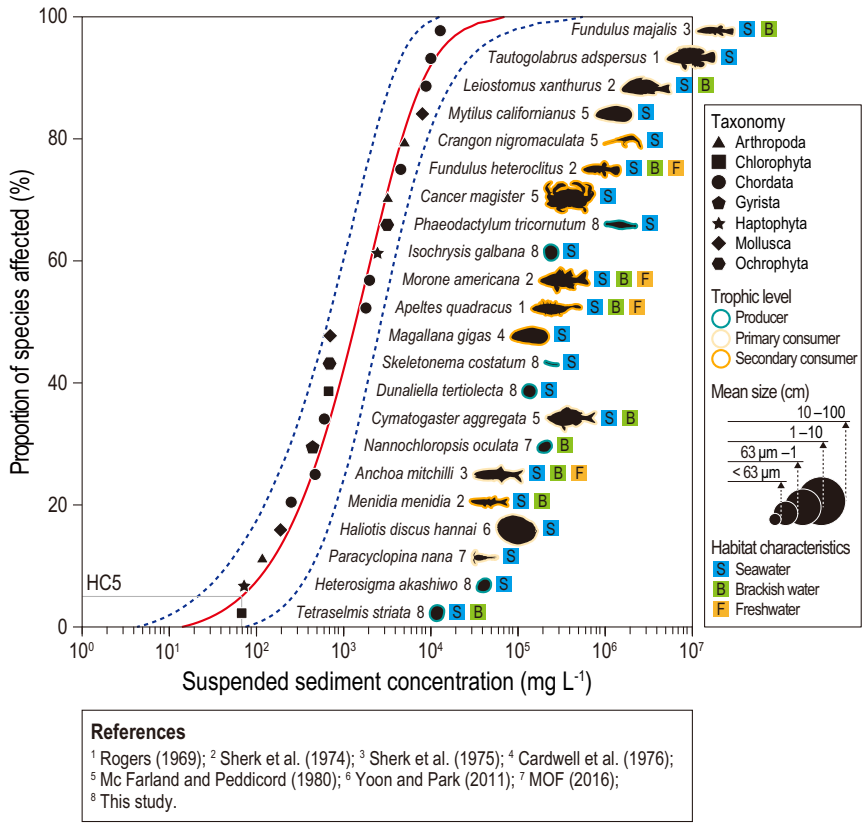

Fig. 5. Species sensitivity distribution (SSD) based on data from this study and others. HC5 represents the hazard concentration for 5 % of the species. Solid line, central tendency; dotted lines, 95 % confidence interval.

conservative approach, as adults are generally less sensitive to SS compared to early developmental stages. However, it is crucial to recognize that organisms in the marine environment exist at various trophic levels and developmental stages. Future research should focus on developing standards that consider only marine species, encompassing their different life stages.

4. Conclusions

Overall, the present study evaluated various endpoints for the ecotoxicity of SS on three marine microalgae species: *D. tertiolecta*, *I. galbana*, and *P. tricornutum*. The findings revealed that exposure to SS had significant adverse effects on these microalgae, notably disrupting vital photosynthetic pathways by altering energy dissipation at the PSII center. A particularly noteworthy outcome was the identification of endpoints that best reflected biological effects observed across diverse microalgae types, including green algae, haptophyte algae, and diatoms. This comprehensive study provides valuable insights into the multiple toxic effects of SS on marine microalgae, emphasizing the necessity of considering multiple endpoints in ecotoxicity assessments. Overall, our findings offer the potential for standardizing methodologies aimed at assessing the risks associated with SS exposure.

CRediT authorship contribution statement

Shin Yeong Park: Writing – original draft, Visualization, Formal analysis, Data curation, Conceptualization. **Junghyun Lee:** Writing – review & editing, Writing – original draft, Visualization, Methodology, Data curation. **Inha Kwon:** Formal analysis, Data curation. **Hyunseo Song:** Formal analysis. **Beomgi Kim:** Formal analysis. **Taewoo Kim:** Data curation. **Changkeun Lee:** Data curation. **Seo Joon Yoon:** Methodology. **Junsung Noh:** Visualization, Data curation. **Seongjin Hong:** Writing – review & editing, Formal analysis, Data curation. **Jong Seong Khim:** Writing – review & editing, Supervision, Project administration, Funding acquisition, Data curation, Conceptualization.

Declaration of competing interest

The authors declare that they have no known competing financial interests or personal relationships that could have appeared to influence the work reported in this paper.

Data availability

Data will be made available on request.

Acknowledgments

This research was supported by “Development of Advanced Science and Technology for Marine Environmental Impact Assessment (RS-2021-KS211469)” and “Development of AI-based Marine Ecosystem Diagnosis and Prediction Technology for Responding and Managing Changes in the Large Marine Ecosystem (202300239887)” of Korea Institute of Marine Science & Technology Promotion (KIMST) funded by the Ministry of Oceans and Fisheries. This work was also supported by the research grant of Kongju National University in 2024 (2024-0293-01).

Appendix A. Supplementary data

Supplementary data to this article can be found online at https://doi.org/10.1016/j.marpolbul.2024.116968.

References

Afrimzon, E., Deutsch, A., Shafran, Y., Zurgil, N., Sandbank, J., Pappo, I., Deutsch, M., 2008. Intracellular esterase activity in living cells may distinguish between metastatic and tumor-free lymph nodes. Clin. Exp. Metastasis 25, 213–224. https://doi.org/10.1007/s10585-007-9135-1.

Almeida, A.C., Gomes, T., Langford, K., Thomas, K.V., Tollefsen, K.E., 2017. Oxidative stress in the algae *Chlamydomonas reinhardtii* exposed to biocides. Aquat. Toxicol. 189, 50–59. https://doi.org/10.1016/j.aquatox.2017.05.014.

Almeida, A.C., Gomes, T., Habuda-Stanić, M., Lomba, J.A.B., Romić, Z., Turkalj, J.V., Lillicrap, A., 2019. Characterization of multiple biomarker responses using flow cytometry to improve environmental hazard assessment with the green microalgae *Raphidocelis subcapitata*. Sci. Total Environ. 687, 827–838. https://doi.org/10.1016/j.scitotenv.2019.06.124.

Almeida, A.C., Gomes, T., Lomba, J.A.B., Lillicrap, A., 2021. Specific toxicity of azithromycin to the freshwater microalga *Raphidocelis subcapitata*. Ecotoxicol. Environ. Safe. 222, 112553 https://doi.org/10.1016/j.ecoenv.2021.112553.

Amiard, J.C., Amiard-Triquet, C., 2015. Conventional risk assessment of environmental contaminants. In: Aquatic Ecotoxicology. Academic Press, pp. 25–49. https://doi.org/10.1016/B978-0-12-800949-9.00002-4.

An, S.-A., Hong, S., Lee, J., Cha, J., Lee, S., Moon, H.-B., Giesy, J.P., Khim, J.S., 2021. Identification of potential toxicants in sediments from an industrialized area in Pohang, South Korea: application of a cell viability assay of microalgae using flow cytometry. J. Hazard. Mater. 405, 124230 https://doi.org/10.1016/j.jhazmat.2020.124230.

Asabonga, M., Cecilia, B., Mpundu, M.C., Vincent, N.M.D., 2017. The physical and environmental impacts of sand mining. Trans. R. Soc. S. Afr. 72 (1), 1–5. https://doi.org/10.1080/0035919X.2016.1209701.

ASTM (American Society for Testing and Materials), 2012. Standard Guide for Conducting Static Toxicity Tests with Microalgae. ASTM International. West Conshohocken, PA pp. E1218–1204.

Bauer, D.E., Conforti, V., Ruiz, L., Gomez, N., 2012. An in situ test to explore the responses of Scenedesmus acutus and Lepocinclis acus as indicators of the changes in water quality in lowland streams. Ecotox. Environ. Saf. 77, 71–78. https://doi.org/10.1016/j.ecoenv.2011.10.021.

Beecraft, L., Watson, S.B., Smith, R.E., 2021. Quantifying the uncertainties in multi-wavelength PAM fluorometry due to innate and irradiance-induced variability of fluorescence spectra. Aquat. Ecol. 55, 169–186. https://doi.org/10.1007/s10452-020-09821-6.

Chapman, P.M., Fairbrother, A., Brown, D., 1998. A critical evaluation of safety (uncertainty) factors for ecological risk assessment. Environ. Toxicol. Chem. 17 (1), 99–108. https://doi.org/10.1002/etc.5620170112.

Chu, S.O., Lee, C., Noh, J., Song, S.J., Hong, S., Ryu, J., Lee, J.-S., Nam, J., Khim, J.S., 2020. Effects of polluted and non-polluted suspended sediments on the oxygen consumption rate of olive flounder. *Paralichthys olivaceus*. Mar. Pollut. Bull. 154, 111113 https://doi.org/10.1016/j.marpolbul.2020.111113.

Chuang, C.Y., Santschi, P.H., Jiang, Y., Ho, Y.F., Quigg, A., Guo, L., Ayranov, M., Schumann, D., 2014. Important role of biomolecules from diatoms in the scavenging of particle-reactive radionuclides of thorium, protactinium, lead, polonium, and beryllium in the ocean: a case study with *Phaeodactylum tricornutum*. Limnol. Oceanogr. 59 (4), 1256–1266. https://doi.org/10.4319/lo.2014.59.4.1256.

Da, S., Le Billon, P., 2022. Sand mining: stopping the grind of unregulated supply chains. Extr. Ind. Soc. 10, 101070 https://doi.org/10.1016/j.exis.2022.101070.

Desbois, A.P., Walton, M., Smith, V.J., 2010. Differential antibacterial activities of fusiform and oval morphotypes of *Phaeodactylum tricornutum* (Bacillariophyceae). J. Mar. Biol. Assoc. United Kingdom 90 (4), 769–774. https://doi.org/10.1017/S0025315409991366.

Dethier, E.N., Silman, M., Leiva, J.D., Alqahtani, S., Fernandez, L.E., Pauca, P., Camalan, S., Tomhave, P., Magilligan, F.J., Renshaw, C.E., Lutz, D.A., 2023. A global rise in alluvial mining increases sediment load in tropical rivers. Nature 620 (7975), 787–793. https://doi.org/10.1038/s41586-023-06309-9.

DIN EN ISO (International Organization for Standardization) 10253, 2018. Water quality-marine algal growth inhibition test with *Skeletonema* sp. and *Phaeodactylum tricornutum*. International Organization for Standardization, Switzerland.

Duce, R.A., Liss, P.S., Merrill, J.T., Atlas, E.L., Buat-Menard, P., Hicks, B.B., Miller, J.M., Ellis, W., Galloway, J.N., Hansen, L., Jickells, T.D., Knap, A.H., Reinhardt, K.H., Schneider, B., Soudine, A., Tokos, J.J., Tsunogai, S., Wollast, R., Zhou, M., 1991. The atmospheric input of trace species to the world ocean. Global Biogeochem. Cy. 5 (3), 193–259. https://doi.org/10.1029/91GB01778.

EC (European Commission), 2011. Common Implementation Strategy for the Water Framework Directive (2000/60/EC) Guidance Document No. 27 Technical Guidance for Deriving Environmental Quality Standards.

Elfwing, T., Tedengre, M., 2002. Effects of copper on the metabolism of three species of tropical oysters, *Saccostrea cucullata*. *Crassostrea lugubris* and *C. belcheri*. Aquaculture 204 (1–2), 157–166. https://doi.org/10.1016/S0044-8486(01)00638-X.

Ene, I.V., Walker, L.A., Schiavone, M., Lee, K.K., Martin-Yken, H., Dague, E., Gow, N.A., Munro, C.A., Brown, A.J., 2015. Cell wall remodeling enzymes modulate fungal cell wall elasticity and osmotic stress resistance. mBio 6 (4), 10–1128. https://doi.org/10.1128/mbio.00986-15.

Esperanza, M., Cid, Á., Herrero, C., Rioboo, C., 2015. Acute effects of a prooxidant herbicide on the microalga *Chlamydomonas reinhardtii*: screening cytotoxicity and genotoxicity endpoints. Aquat. Toxicol. 165, 210–221. https://doi.org/10.1016/j.aquatox.2015.06.004.

Franklin, N.M., Stauber, J.L., Lim, R.P., 2001. Development of flow cytometry-based algal bioassays for assessing toxicity of copper in natural waters. Environ. Toxicol. Chem. Int. J. 20, 160–170. https://doi.org/10.1002/etc.5620200118.

Gallo, C., d'Ippolito, G., Nuzzo, G., Sardo, A., Fontana, A., 2017. Autoinhibitory sterol sulfates mediate programmed cell death in a bloom-forming marine diatom. Nat. Commun. 8, 1292. https://doi.org/10.1038/s41467-017-01300-1.

Gao, P., Li, Z., Gibson, M., Gao, H., 2014. Ecological risk assessment of nonylphenol in coastal waters of China based on species sensitivity distribution model. Chemosphere 104, 113–119. https://doi.org/10.1016/j.chemosphere.2013.10.076.

Garcia, M.H., 2008. Sedimentation engineering: processes, measurements, modeling and practice. ASCE Manuals and Reports on Engineering Practice No. 110. ASCE Pub. doi:https://doi.org/10.1061/9780784408148.

Gomes, T., Almeida, A.C., Georgantzopoulou, A., 2020. Characterization of cell responses in *Rhodomonas baltica* exposed to PMMA nanoplastics. Sci. Total Environ. 726, 138547 https://doi.org/10.1016/j.scitotenv.2020.138547.

Gredelj, A., Barausse, A., Grechi, L., Palmeri, L., 2018. Deriving predicted no-effect concentrations (PNECs) for emerging contaminants in the river Po, Italy, using three approaches: assessment factor, species sensitivity distribution and AQUATOX ecosystem modelling. Environ. Internat. 119, 66–78. https://doi.org/10.1016/j.envint.2018.06.017.

Hackney, C., Vasilopoulos, G., Heng, S., Darbari, V., Walker, S., Parsons, D., 2021. Sand mining far outpaces natural supply in a large alluvial river. Earth Surface Dynamics Discussions. 1–20 https://doi.org/10.5194/esurf-9-1323-2021.

Hess, F.D., 2000. Light-dependent herbicides: an overview. Weed Sci. 48, 160–170. https://doi.org/10.1614/0043-1745(2000)048[0160:LDHAO]2.0.CO;2.

Imai, I., Inaba, N., Yamamoto, K., 2021. Harmful algal blooms and environmentally friendly control strategies in Japan. Fish. Sci. 87 (4), 437–464. https://doi.org/10.1007/s12562-021-01524-7.

Johnson, G.N., Young, A.J., Scholes, J.D., Horton, P., 1993. The dissipation of excess excitation energy in British plant species. Plant Cell Environ. 16, 673–679. https://doi.org/10.1111/j.1365-3040.1993.tb00485.x.

Joshi, S.S., Vitankar, V.S., Dalvi, V.H., Joshi, J.B., 2023. Solid suspension and solid-liquid mass transfer in stirred reactors. In: Handbook of Multiphase Flow Science and Technology. Springer Nature Singapore, Singapore, pp. 1491–1553. https://doi.org/10.1007/978-981-287-092-6_49.

Juneau, P., Popovic, R., 1999. Evidence for the rapid phytotoxicity and environmental stress evaluation using the PAM fluorometric method: importance and future application. Ecotoxicology 8, 449–455. https://doi.org/10.1023/A:1008955819527.

Kramer, D.M., Johnson, G., Kiirats, O., Edwards, G.E., 2004. New fluorescence parameters for the determination of QA redox state and excitation energy fluxes. Photosynth. Res. 79, 209–218. https://doi.org/10.1023/B:PRES.0000015391.99477.0d.

Kwon, H.K., 2013. A Study on Phytoremediation of Eutrphic Coastal Sediments Using Benthic Microalgae and Light Emitting Diode. Ph. D. Thesis,. Pukyung National University, Busan, p. 255.

Lee, J., Choi, E.J., Rhie, K., 2015. Validation of algal viability treated with total residual oxidant and organic matter by flow cytometry. Mar. Pollut. Bull. 97 (1–2), 95–104. https://doi.org/10.1016/j.marpolbul.2015.06.029.

Lee, J., Hong, S., Kim, T., Lee, C., An, S.-A., Kwon, B.-O., Lee, S., Moon, H.-B., Giesy, J.P., Khim, J.S., 2020. Multiple bioassays and targeted and nontargeted analyses to characterize potential toxicological effects associated with sediments of Masan Bay: focusing on AhR-mediated potency. Environ. Sci. Technol. 54, 4443–4454. https://doi.org/10.1021/acs.est.9b07390.

Lee, J., Hong, S., An, S-A., Khim, J.S., 2023. Methodological advances and future directions of microalgal bioassays for evaluation of potential toxicity in environmental samples: a review. Environ. Internat. 173, 107869. doi:https://doi.org/10.1016/j.envint.2023.107869.

Li, J., Schiavo, S., Rametta, G., Miglietta, M.L., La Ferrara, V., Wu, C., Manzo, S., 2017. Comparative toxicity of nano ZnO and bulk ZnO towards marine algae *Tetraselmis suecica* and *Phaeodactylum tricornutum*. Environ. Sci. Pollut. Res. 24, 6543–6553. https://doi.org/10.1007/s11356-016-8343-0.

Liu, G., Chai, X., Shao, Y., Hu, L., Xie, Q., Wu, H., 2011. Toxicity of copper, lead, and cadmium on the motility of two marine microalgae *Isochrysis galbana* and *Tetraselmis chui*. J. Environ. Sci. 23 (2), 330–335. https://doi.org/10.1016/S1001-0742(10)60410-X.

Long, E.R., MacDonald, D.D., Smith, L., Calder, F.D., 1995. Incidence of adverse biological effects within ranges of chemical concentrations in marine and estuarine sediments. Environ. Manag. 19, 81–97. https://doi.org/10.1007/BF02472006.

Long, E.R., MacDonald, D.D., Recommended uses of empirically derived sediment quality guidelines for marine and estuarine ecosystems, 1998. Hum. Ecol. Risk. Assess. 4, 1019–1039. https://doi.org/10.1080/10807039891284956.

Machado, M.D., Soares, E.V., 2012. Development of a short-term assay based on the evaluation of the plasma membrane integrity of the alga *Pseudokirchneriella subcapitata*. Appl. Microbiol. Biotechnol. 95, 1035–1042. https://doi.org/10.1007/s00253-012-4185-y.

Magnusson, M., Heimann, K., Negri, A.P., 2008. Comparative effects of herbicides on photosynthesis and growth of tropical estuarine microalgae. Mar. Pollut. Bull. 56, 1545–1552. https://doi.org/10.1016/j.marpolbul.2008.05.023.

Metaxas, A., Lewis, A.G., 1991. Copper tolerance of *Skeletonema costatum* and *Nitzschia thermalis*. Aqua. Toxic. 19, 265–280. https://doi.org/10.1016/0166-445X(91)90052-B.

Míguez, L., Esperanza, M., Seoane, M., Cid, Á., 2021. Assessment of cytotoxicity biomarkers on the microalga *Chlamydomonas reinhardtii* exposed to emerging and priority pollutants. Ecotoxicol. Environ. Saf. 208, 111646 https://doi.org/10.1016/j.ecoenv.2020.111646.

MOF (Ministry of Oceans and Fisheries), 2016. Standardized bioassay test for fishery damage investigation, Korea.

MOF (Ministry of Oceans and Fisheries), 2018. Marine environment quality standards. Korea.

Murchie, E.H., Lawson, T., 2013. Chlorophyll fluorescence analysis: a guide to good practice and understanding some new applications. J. Exper. Bot. 64, 3983–3998. https://doi.org/10.1093/jxb/ert208.

Nestler, H., Groh, K.J., Schonenberger, R., Behra, R., Schirmer, K., Eggen, R.I., Suter, M. J.-F., 2012. Multiple-endpoint assay provides a detailed mechanistic view of responses to herbicide exposure in *Chlamydomonas reinhardtii*. Aquat. Toxicol. 110, 214–224. https://doi.org/10.1016/j.aquatox.2012.01.014.

Newcombe, C., Macdonald, D., 1991. Effects of suspended sediments on aquatic ecosystems. N. Am. J. Fish. Manage. 11, 72–82. https://doi.org/10.1577/1548-8675(1991)011%3C0072:EOSSOA%3E2.3.CO;2.

Nichols, M., Diaz, R.J., Schaffner, L.C., 1990. Effects of hopper dredging and sediment dispersion. Chesapeake Bay. Environ. Geol. Water Sci. 15, 31–43. https://doi.org/10.1007/BF01704879.

Olsen, R.O., Hess-Erga, O.K., Larsen, A., Hoffmann, F., Thuestad, G., Hoell, I.A., 2016. Dual staining with CFDA-AM and SYTOX blue in flow cytometry analysis of UV-irradiated Tetraselmis suecica to evaluate vitality. Aquat. Biol. 25, 39–52. https://doi.org/10.3354/ab00662.

Overnell, J., 1975. The effect of heavy metals on photosynthesis and loss of cell potassium in two species of marine algae, *Dunaliella tertiolecta* and *Phaeodactylum tricornutum*. Mar. Biol. 29 (1), 99–103. https://doi.org/10.1007/BF00395531.

Patrinou, V., Patsialou, S., Daskalaki, A., Economou, C.N., Aggelis, G., Vayenas, D.V., Tekerlekopoulou, A.G., 2023. Laboratory-and pilot-scale cultivation of *Tetraselmis striata* to produce valuable metabolic compounds. Life 13 (2), 480. https://doi.org/10.3390/life13020480.

Pollock, F., Lamb, Joleah, Field, S., Heron, S., Schaffelke, B., Shedrawi, G., Bourne, D., Willis, B., 2014. Sediment and turbidity associated with offshore dredging increase coral disease prevalence on nearby reefs. PloS One 9 (7), 102498. https://doi.org/10.1371/journal.pone.0102498.

Ranjbarfordoei, A., Samson, R., Damme, P.V., 2006. Chlorophyll fluorescence performance of sweet almond [[*Prunus dulcis* (Miller)] D. Webb] in response to salinity stress induced by NaCl. Photosynthetica 44, 513–522. https://doi.org/10.1007/s11099-006-0064-z.

Schreiber, U., Quayle, P., Schmidt, S., Escher, B.I., Mueller, J.F., 2007. Methodology and evaluation of a highly sensitive algae toxicity test based on multiwell chlorophyll fluorescence imaging. Biosens. Bioelectron. 22, 2554–2563. https://doi.org/10.1016/j.bios.2006.10.018.

Schüler, L.M., Bombo, G., Duarte, P., Santos, T.F., Maia, I.B., Pinheiro, F., Marques, J., Jacinto, R., Schulze, P.S.C., Pereira, H., Barreira, L., Varela, J.C., 2021. Carotenoid biosynthetic gene expression, pigment and n-3 fatty acid contents in carotenoid-rich *Tetraselmis striata* CTP4 strains under heat stress combined with high light. Bioresour. Technol. 337, 125385 https://doi.org/10.1016/j.biortech.2021.125385.

Schulze, P.S., Hulatt, C.J., Morales-Sánchez, D., Wijffels, R.H., Kiron, V., 2019. Fatty acids and proteins from marine cold adapted microalgae for biotechnology. Algal Res. 42, 101604 https://doi.org/10.1016/j.algal.2019.101604.

Utne-Palm, A.C., 2002. Visual feeding of fish in a turbid environment: physical and behavioural aspects. Mar. Fresh. Behav. Physiol. 35 (1–2), 111–128. https://doi.org/10.1080/10236240290025644.

Vieira, L.R., Guilhermino, L., 2012. Multiple stress effects on marine planktonic organisms: influence of temperature on the toxicity of polycyclic aromatic hydrocarbons to *Tetraselmis chuii*. J. Sea Res. 72, 94–98. https://doi.org/10.1016/j.seares.2012.02.004.

Wang, R., Liu, Q., 2022. Responses of bloom-forming *heterosigma akashiwo* to allelochemical linoleic acid: growth inhibition, oxidative stress and apoptosis. Front. Mar. Sci. 8, 793567 https://doi.org/10.3389/fmars.2021.793567.

Wang, J., Zhang, Y., Li, H., Cao, J., 2013. Competitive interaction between diatom *Skeletonema costatum* and dinoflagellate *Prorocentrum donghaiense* in laboratory culture. J. Plankton Res. 35 (2), 367–378. https://doi.org/10.1093/plankt/fbs098.

Wang, X.-X., Zhang, T.-Y., Dao, G.-H., Xu, Z.-B., Wu, Y.-H., Hu, H.-Y., 2020. Assessment and mechanisms of microalgae growth inhibition by phosphonates: effects of intrinsic toxicity and complexation. Water Res. 186, 116333 https://doi.org/10.1016/j.watres.2020.116333.

Wang, D., de los Reyes III, F.L., Ducoste, J.J., 2023. Microplate-based cell viability assay as a cost-effective alternative to flow cytometry for microalgae analysis. Environ. Sci. Technol. 57 (50), 21200–21211. https://doi.org/10.1021/acs.est.3c05675.

Warne, M.St.J., Batley, G.E., van Dam, R.A., Chapman, J.C., Fox, D.R., Hickey, C.W., Stauber, J.L., 2018. Revised Method for Deriving Australian and New Zealand Water Quality Guideline Values for Toxicants. Queensland Department of Science, Information Technology and Innovation. http://nla.gov.au/nla.obj-2742606044.

Wei, Y., Zhu, N., Lavoie, M., Wang, J., Qian, H., Fu, Z., 2014. Copper toxicity to *Phaeodactylum tricornutum*: a survey of the sensitivity of various toxicity endpoints at the physiological, biochemical, molecular and structural levels. Biometals 27, 527–537. https://doi.org/10.1007/s10534-014-9727-6.

Wenger, A.S., Johansen, J.L., Jones, G.P., 2012. Increasing suspended sediment reduces foraging, growth and condition of a planktivorous damselfish. J. Exp. Mar. Bio. Ecol. 428, 43–48. https://doi.org/10.1016/j.jembe.2012.06.004.

Xu, F., Li, Y.-L., Wang, Y., He, W., Kong, X.-Z., Qin, N., Liu, W.-X., Wu, W.-J., Erik, S.E., 2015. Key issues for the development and application of the species sensitivity distribution (SSD) model for ecological risk assessment. Ecol. Indic. 54, 227–237. https://doi.org/10.1016/j.ecolind.2015.02.001.

Yamada, M., Otsubo, M., Tsutsumi, Y., Mizota, C., Iida, N., Okamura, K., Kodama, M., Umehara, A., 2013. Species diversity of the marine diatom genus *Skeletonema* in Japanese brackish water areas. Fish. Sci. 79, 923–934. https://doi.org/10.1007/s12562-013-0671-0.

Yamasaki, Y., Fujita, M., Kawano, S., Baba, T., 2018. Effect of salinity on interspecific competition between the dinoflagellate *Alexandrium catenella* and the raphidophyte *Heterosigma akashiwo*. Aquat. Microb. Ecol. 81 (1), 73–82. https://doi.org/10.3354/ame01860.

Yeh, T.Y., Ke, T.Y., Lin, Y.L., 2011. Algal growth control within natural water purification systems: macrophyte light shading effects. Water Air Soil Pollut. 214, 575–586. https://doi.org/10.1007/s11270-010-0447-4.

<Supplementary Materials>

Ecotoxicological effects of suspended sediments on marine microalgae using flow cytometry and pulse-amplitude modulation (PAM) fluorometry

Shin Yeong Park, Junghyun Lee *, Inha Kwon, Hyunseo Song, Beomgi Kim, Taewoo Kim, Changkeun Lee, Seo Joon Yoon, Junsung Noh, Seongjin Hong, Jong Seong Khim *

This file includes:

Number of pages: 13

Number of Supplementary Tables: 8, Tables S1 to S8

Number of Supplementary Figures: 3, Figs. S1 to S3

References

***Corresponding authors.**
E-mail addresses: leejunghyun@kongju.ac.kr (J. Lee); jskocean@snu.ac.kr (J.S. Khim).

Supplementary Tables

Table S1. Culture conditions and bioassay protocol for the six microalgae.

Scientific name	***Dunaliella tertiolecta***	***Isochrysis galbana***	***Phaeodactylum triconutum***	***Tetraselmis striata***	***Heterosigma akashiwo***	***Skeletonema costatum***
Cell characteristics						
Class	Chlorophyceae	Prymnesiophyceae	Bacillariophyceae	Chlorophyceae	Prymnesiophyceae	Bacillariophyceae
Cell size	6−14 μm	5−6 μm	5−6 μm × 10−14 μm	4–25 μm	18–34 μm	2–21 × 2–61 μm
Culture/test incubation condition						
Temperature	20 ℃					
Photoperiod	12:12 (Light : Dark)					
Shaking speed	100 rpm					
Culture media	f/2 medium + autoclaved seawater (121 ℃)					
Toxicity testing parameters						
Initial cell density	3×10^4 cells mL^{-1}	9×10^4 cells mL^{-1}	7×10^4 cells mL^{-1}	5×10^4 cells mL^{-1}	5×10^4 cells mL^{-1}	5×10^4 cells mL^{-1}
Test type	Static non-renewal					
Test duration	96 h					
Test chamber	250 mL culture flask					
Test solution volume	100 mL					

Table S2. Staining and instrumental conditions for flow cytometry.

Endpoint	**Stain Dye**	**Target features**	**Concentration (Exposure time)**			**Positive control**	**Laser**	**Detector**
			D. tertiolecta	***I. galbana***	***P. tricornutum***			
Esterase activity	Fluorescein diacetate (FDA)	Non-specific esterase	20 µM (20 min)	5 µM (15 min)	20 µM (20 min)	Heat-treat dead (60 °C, 1 h)	488 nm	FITC (530/30 nm)
Cell membrane intensity	SYTOX Blue	RNA/ DNA	-	2 µM (10 min)	-	Heat-treat dead (60 °C, 1 h)	405 nm	Pacific Blue (450/50 nm)
	Propidium iodide (PI)	DNA	10 µM (30 min)	-	10 µM (30 min)		488 nm	PE (585/42 nm)
Chlorophyll-a	-	Cell feature	-	-	-	-	633 nm	APC (660/20 nm)
Cell size	-	Cell feature	-	-	-	-	488 nm	FS
Intracellular complex	-	Cell feature	-	-	-	-	488 nm	SS

Table S3. Overview of the quadrants (Q1−Q4) in response to elevated (+) and low (−) fluorescence intensity when cells were stained with FDA and SYTOX blue (Olsen et al., 2016).

Quadrant	FDA	SYTOX blue	Physiological characteristics	Vitality
Q1	+	–	Esterase active; membrane intact	Healthy
Q2	+	+	Esterase active; membrane damaged	Severely damaged
Q3	–	–	Esterase inactive; membrane intact or DNA/RNA degraded	Severely damaged
Q4	–	+	Esterase inactive; membrane damaged	Stressed

Table S4. Fluorescence parameters calculated from imaging-PAM fluorometry measurements for three microalgae.

Parameter	Definition	Equation	Reference
Fo’	Minimum fluorescence in light-adapted state	Fo/(Fv/Fm + Fo/Fm')	Oxborough and Baker (1997)
Fm’	Maximum fluorescence in light-adapted state	-	-
Y(II)	Effective PS II quantum yield	(Fm'-F)/Fm'	Genty et al. (1989)
Y(NPQ)	Quantum yield of regulated energy dissipation	1 - Y(II) - 1/(NPQ+1+qL(Fm/Fo-1))	Kramer et al. (2004)
Y(NO)	Quantum yield of non-regulated energy dissipation	1/(NPQ+1+qL(Fm/Fo-1))	Kramer et al. (2004)
qN	Coefficient of non-photochemical quenching	(Fm-Fm')/(Fm-Fo')*	Schreiber et al. (1986); Juneau and Popovic (1999)
qL	Coefficient of photochemical quenching	(Fm'-F)/(Fm'-Fo') × Fo'/F = qP × Fo'/F*	Kramer et al. (2004)
qP	Coefficient of photochemical quenching	(Fm’-F)/(Fm’-Fo’)*	Schreiber et al. (1986); Juneau and Popovic (1999)
$_{max}$ETR	Maximum photosynthetic electron transport rate	0.5 x Y(II) × PAR x I_A**	Genty et al. (1989)

* Fo' parameter estimated using the approximation of Oxborough and Baker (1997): Fo' = Fo/(Fv/Fm + Fo/Fm').

**Where 0.5 is a factor that assumes equal distribution of energy between PSII and PSI, PAR is the actinic photosynthetically active radiation generated by IMAGING PAM and I_A is the assumed absorbance by the photosynthetic organism (0.84).

Table S5. Concentrations of metals in water column of SS treatment (100 and 10,000 mg L^{-1}). It is assumed that 100% of the metals in sediments collected from the West Sea Exclusive Economic Zone sand mining complex were leached into seawater.

	Li	**Cr(VI)**	**Ni**	**Cu**	**Zn**	**As**	**Pb**	**Cd**	**Hg**
Concentration of heavy metals eluted in 100 mg L^{-1}									
Mean	0.07	0.07	0.02	0.01	0.08	0.01	0.16	0.0003	0.0006
± Std. (μg L^{-1})	± 0.002	± 0.002	± 0.0005	± 0.001	± 0.002	± 0.001	± 0.001	± 0.00002	± 0.00004
Concentration of heavy metals eluted in 10,000 mg L^{-1}									
Mean	7.0	7.2	2.5	1.5	7.5	1.4	16.2	0.03	0.06
± Std. (μg L^{-1})	± 0.2	± 0.2	± 0.05	± 0.1	± 0.2	± 0.1	± 0.1	± 0.002	± 0.004
Water quality guidelines of heavy metals for protection of aquatic life									
Marine Environmental Standards (μg L^{-1})[a]	11.0	200.0	11.0	3.0	34.0	-	7.6	19.0	1.8
EPA (μg L^{-1})	-	-	-	-	-	-	10.0	10.0	-
EU (μg L^{-1})	-	-	-	-	-	10.0	10.0	5.0	10.0

[a] Ministry of Oceans and Fisheries (MOF), 2018. Marine Environment Quality Standards, Korea.

Table S6. Pearson's correlations between the endpoints of *Dunaliella tertiolecta*. Bold values denote statistical significance at the $p < 0.05$ level (* and ** indicate that correlation is significant at the 0.05 and 0.01, respectively).

	GI [a]	EA [b]	CMI [c]	Chl-*a* [d]	CS [e]	IC [f]	Fo'	Fm'	Y(II)	Y(NPQ)	Y(NO)	qN	qL	qP	$_{max}$ETR [g]
GI	-														
EA	**-0.802****	-													
CMI	**0.622****	**-0.781****	-												
Chl-*a*	**-0.834****	**0.969****	**-0.649****	-											
CS	**-0.814****	**0.689****	**-0.533***	**0.733****	-										
IC	**-0.717****	**0.896****	**-0.544***	**0.920****	**0.802****	-									
Fo'	**-0.943****	**0.765****	**-0.678****	**0.800****	**0.811****	**0.639****	-								
Fm'	**-0.943****	**0.763****	**-0.670****	**0.800****	**0.803****	**0.633****	**0.999****	-							
Y(II)	**0.821****	**-0.522***	**0.469***	**-0.583***	**-0.699****	-0.413	**-0.914****	**-0.919****	-						
Y(NPQ)	**-0.877****	**0.656****	-0.322	**0.750****	**0.732****	**0.637****	**0.826****	**0.835****	**-0.765****	-					
Y(NO)	-0.451	0.198	-0.440	0.203	0.407	0.049	**0.644****	**0.642****	**-0.807****	0.244	-				
qN	**-0.888****	**0.652****	-0.348	**0.746****	**0.746****	**0.619****	**0.855****	**0.864****	**-0.792****	**0.996****	0.293	-			
qL	**0.800****	**-0.497***	0.460	**-0.558***	**-0.674****	-0.382	**-0.900****	**-0.906****	**0.996****	**-0.742****	**-0.827****	**-0.770****	-		
qP	**0.841****	**-0.539***	**0.496***	**-0.600****	**-0.728****	-0.432	**-0.935****	**-0.939****	**0.994****	**-0.780****	**-0.796****	**-0.810****	**0.993****	-	
$_{max}$ETR	**0.787****	**-0.492***	**0.490***	**-0.542***	**-0.663****	-0.367	**-0.893****	**-0.899****	**0.981****	**-0.690****	**-0.859****	**-0.721****	**0.990****	**0.982****	-

[a] Growth inhibition (GI). [b] Esterase activity (EA). [c] Cell membrane intensity (CMI). [d] Chlorophyll-*a* (Chl-*a*). [e] Cell size (CS). [f] Intracellular complexity (IC). [g] Electron transfer rate (ETR).

Table S7. Pearson's correlations between the endpoints of *Isochrysis galbana*. Bold values denote statistical significance at the $p < 0.05$ level (* and ** indicate that correlation is significant at the 0.05 and 0.01, respectively).

	GI [a]	EA [b]	CMI [c]	Chl-*a* [d]	CS [e]	IC [f]	Fo'	Fm'	Y(II)	Y(NPQ)	Y(NO)	qN	qL	qP	$_{max}$ETR [g]
GI	-														
EA	**-0.830****	-													
CMI	**-0.884****	**0.936****	-												
Chl-*a*	**-0.897****	**0.937****	**0.917****	-											
CS	**-0.793****	**0.989****	**0.906****	**0.912****	-										
IC	**-0.803****	**0.949****	**0.893****	**0.946****	**0.945****	-									
Fo'	**-0.946****	**0.874****	**0.892****	**0.963****	**0.839****	**0.876****	-								
Fm'	**-0.944****	**0.871****	**0.892****	**0.961****	**0.836****	**0.872****	**1.000****	-							
Y(II)	**0.864****	**-0.571***	**-0.680****	**-0.676****	**-0.525***	**-0.562***	**-0.794****	**-0.792****	-						
Y(NPQ)	**-0.724****	**0.613****	**0.702****	**0.673****	**0.567***	**0.621****	**0.675****	**0.669****	**-0.821****	-					
Y(NO)	-0.085	-0.177	-0.154	-0.113	-0.170	-0.198	0.060	0.067	-0.121	-0.465	-				
qN	**-0.726****	**0.595****	**0.688****	**0.668****	**0.547***	**0.608****	**0.683****	**0.677****	**-0.841****	**0.996****	-0.428	-			
qL	**0.850****	**-0.548***	**-0.665****	**-0.654****	**-0.503***	**-0.534***	**-0.786****	**-0.785****	**0.991****	**-0.759****	-0.216	**-0.780****	-		
qP	**0.851****	**-0.566***	**-0.672****	**-0.665****	**-0.523***	**-0.557***	**-0.775****	**-0.772****	**0.996****	**-0.839****	-0.086	**-0.857****	**0.984****	-	
$_{max}$ETR	**0.839****	**-0.567***	**-0.670****	**-0.693****	**-0.526***	**-0.563***	**-0.822****	**-0.827****	**0.860****	**-0.510***	-0.445	**-0.529***	**0.905****	**0.827****	-

[a] Growth inhibition (GI). [b] Esterase activity (EA). [c] Cell membrane intensity (CMI). [d] Chlorophyll-*a* (Chl-*a*). [e] Cell size (CS). [f] Intracellular complexity (IC). [g] Electron transfer rate (ETR).

Table S8. Pearson's correlations between the endpoints of *Phaeodactylum tricornutum*. Bold values denote statistical significance at the $p < 0.05$ level (* and ** indicate that correlation is significant at the 0.05 and 0.01, respectively).

	GI [a]	EA [b]	CMI [c]	Chl-*a* [d]	CS [e]	IC [f]	Fo'	Fm'	Y(II)	Y(NPQ)	Y(NO)	qN	qL	qP	$_{max}$ETR [g]
GI	-														
EA	**-0.869****	-													
CMI	0.197	0.070	-												
Chl-*a*	**-0.819****	**0.941****	0.323	-											
CS	**-0.568***	**0.763****	0.410	**0.827****	-										
IC	0.155	0.108	**0.888****	0.298	0.187	-									
Fo'	**-0.846****	**0.921****	0.303	**0.984****	**0.768****	0.305	-								
Fm'	**-0.846****	**0.925****	0.301	**0.986****	**0.772****	0.300	**0.999****	-							
Y(II)	**0.872****	**-0.860****	-0.002	**-0.847****	**-0.645****	0.013	**-0.877****	**-0.874****	-						
Y(NPQ)	**-0.566***	**0.719****	0.314	**0.769****	**0.679****	0.323	**0.770****	**0.767****	**-0.738****	-					
Y(NO)	-0.300	0.076	-0.438	-0.015	-0.143	**-0.470***	0.017	0.017	-0.227	**-0.486***	-				
qN	**-0.571***	**0.730****	0.318	**0.778****	**0.683****	0.331	**0.781****	**0.777****	**-0.751****	**0.999****	-0.465	-			
qL	**0.881****	**-0.855****	0.030	**-0.836****	**-0.622****	0.046	**-0.866****	**-0.864****	**0.992****	**-0.690****	-0.292	**-0.704****	-		
qP	**0.839****	**-0.845****	-0.013	**-0.832****	**-0.644****	0.012	**-0.858****	**-0.855****	**0.996****	**-0.741****	-0.224	**-0.757****	**0.991****	-	
$_{max}$ETR	**0.926****	**-0.845****	-0.003	**-0.842****	**-0.540***	-0.045	**-0.885****	**-0.887****	**0.900****	**-0.550***	-0.369	**-0.561***	**0.926****	**0.877****	-

[a] Growth inhibition (GI). [b] Esterase activity (EA). [c] Cell membrane intensity (CMI). [d] Chlorophyll-*a* (Chl-*a*). [e] Cell size (CS). [f] Intracellular complexity (IC). [g] Electron transfer rate (ETR).

Supplementary Figures

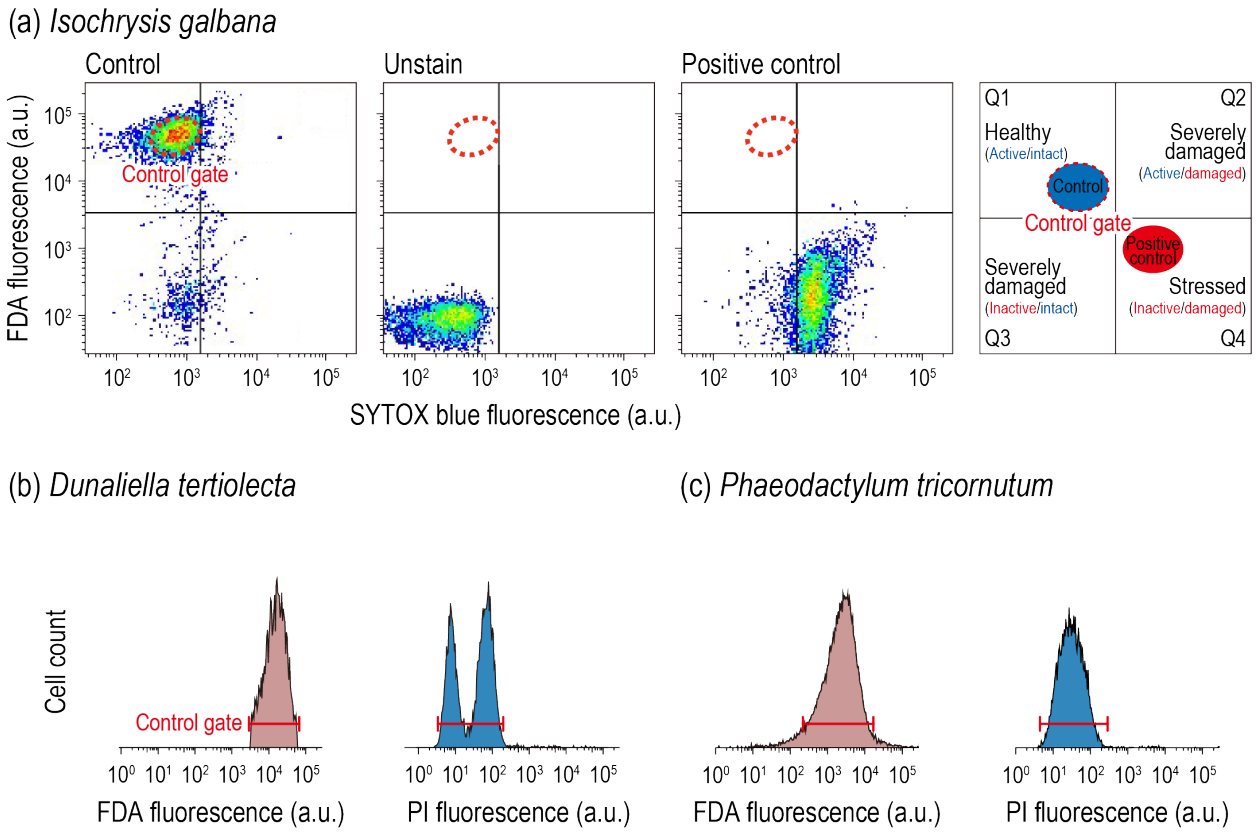

Fig. S1. (a) Bi-dimensional cytograms of the double staining of control cells for *Isochrysis galbana* and **(b)** control gate of single staining for *Dunaliella tertiolecta* and *Phaeodactylum tricornutum*.

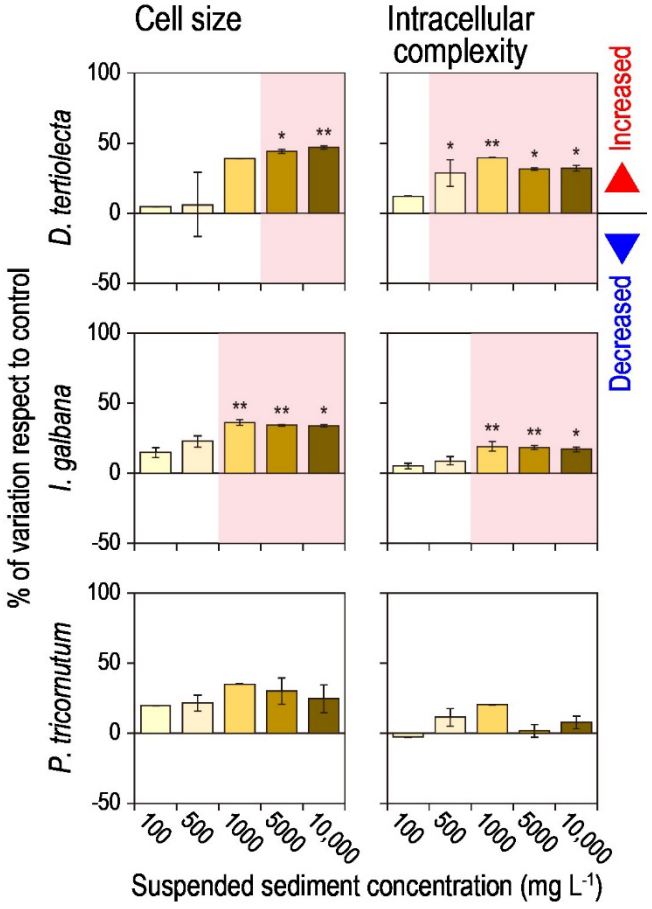

Fig. S2. Cell size and cell membrane intensity for *Dunaliella tertiolecta*, *Isochrysis galbana*, and *Phaeodactylum tricornutum* exposed to suspended sediment. All endpoints are expressed in arbitrary units (a.u.). Data (mean ± standard deviation) represent results from three replicates (* and ** represent significantly different compared by control $p < 0.05$ and $p < 0.01$, respectively). Red shading indicates a significant difference ($p < 0.05$) compared to the control group.

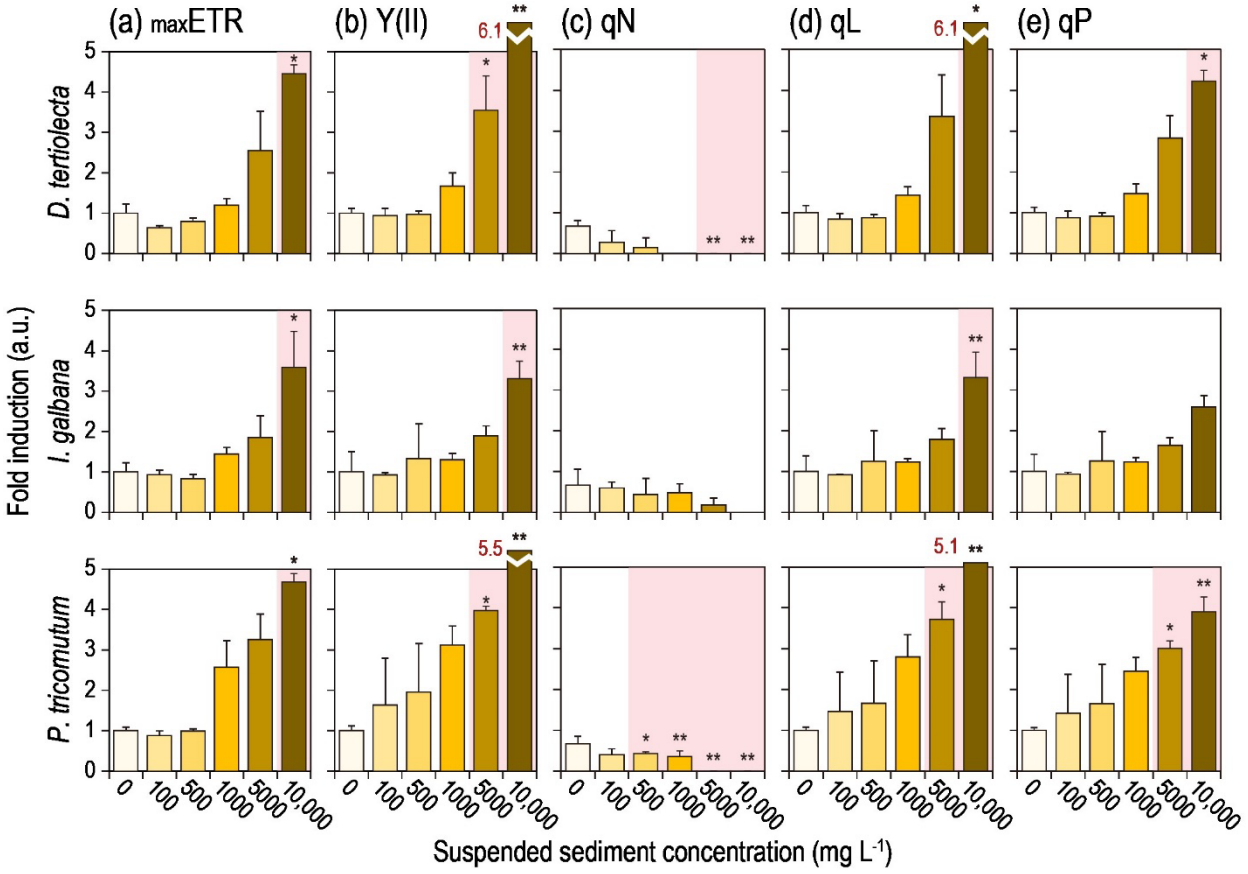

Fig. S3. Photosystem II parameters for *Dunaliella tertiolecta*, *Isochrysis galbana*, and *Phaeodactylum tricornutum* exposed to suspended sediments. **(a)** $_{max}$ETR – maximum photosynthetic electron transport rate; **(b)** Y(II) – Effective PS II quantum yield; **(c)** qN – Coefficient of non-photochemical quenching; **(d)** qL or **(e)** qP – Coefficient of photochemical quenching. All endpoints are expressed in arbitrary units (a.u.). Data (mean ± standard deviation) represent results from three replicate experiments (* and ** represent significantly different compared by control $p < 0.05$ and $p < 0.01$, respectively). Red shading indicates a significant difference ($p < 0.05$) compared to the control group.

References

Genty, B., Briantais, J.-M., Baker, N.R., 1989. The relationship between the quantum yield of photosynthetic electron transport and quenching of chlorophyll fluorescence. Bioch. Biophys. Acta. 990, 87–92.

Schreiber, U., Schliwa, U., Bilger, W., 1986. Continuous recording of photochemical and non-photochemical chlorophyll fluorescence quenching with a new type of modulation fluorometer. Photosynth. Res. 10, 51–62.

Juneau, P., Popovic, R., 1999. Evidence for the rapid phytotoxicity and environmental stress evaluation using the PAM fluorometric method: importance and future application. Ecotox. 8, 449–455.

Ministry of Oceans and Fisheries (MOF), 2018. Marine Environment Quality Standards, Korea.

Olsen, R.O., Hess-Erga, O.K., Larsen, A., Hoffmann, F., Thuestad, G., Hoell, I.A., 2016. Dual staining with CFDA-AM and SYTOX blue in flow cytometry analysis of UVirradiated Tetraselmis suecica to evaluate vitality. Aquat. Biol. 25, 39–52

Oxborough, K., Baker, N.R. 1997. Resolving chlorophyll a fluorescence images of photosynthetic efficiency into photochemical and non-photochemical components - calcutation of qP and F´v/F´m without measuring F´0. Photosynth Res. 54: 135–142.

Kramer, D.M., Johnson, G., Kiirats, O., Edwards, G.E. 2004. New fluorescence parameters for the determination of QA redox state and excitation energy fluxes. Photosynth. Res. 79: 209–218.